Front. Phys. 13(2), 134202 (2018)
https://doi.org/10.1007/s11467-017-0719-1

RESEARCH ARTICLE

Slow light effect with high group index and wideband by saddle-like mode in PC-CROW

Yong Wan[1], Li-Jun Jiang[2], Sheng Xu[1], Meng-Xue Li[1], Meng-Nan Liu[1], Cheng-Yi Jiang[1], Feng Yuan[1,†]

[1] *College of Physics Science, Qingdao University, Qingdao 266071, China*
[2] *Qingdao No. 2 Middle School of Shandong Province, Qingdao 266071, China*
Corresponding author. E-mail: [†] *yuan@qdu.edu.cn*
Received April 4, 2017; accepted May 23, 2017

Slow light with high group index and wideband is achieved in photonic crystal coupled-resonator optical waveguides (PC-CROWs). According to the eye-shaped scatterers and various microcavities, saddle-like curves between the normalized frequency f and wave number k can be obtained by adjusting the parameters of the scatterers, parameters of the coupling microcavities, and positions of the scatterers. Slow light with decent flat band and group index can then be achieved by optimizing the parameters. Simulations prove that the maximal value of the group index is $> 10^4$, and the normalized delay bandwidth product within a new varying range of $n_g > 10^2$ or $n_g > 10^3$ can be a new and effective criterion of evaluation for the slow light in PC-CROWs.

Keywords eye-shaped scatterer, slow light, photonic crystal, coupled-resonator optical waveguide

PACS numbers 42.82. Et, 42.15. Eq, 42.70. Qs

1 Introduction

Slow light with ultra-low group velocity has extensive potential applications in many areas, such as optical delay lines, all-optical buffers, laser technology, solar energy, and photocatalysis [1–6]. These applications are essential for all-optical communications and signal-processing systems, and as one of the most practical methods for slow light generation, the use of photonic crystal (PC) waveguides has multiple advantages [7–9]. Compared with the conventional PC line-defect waveguide (PCW), the PC coupled-resonator optical waveguide (PC-CROW) produces slow light with a far smaller group velocity [10, 11], which is desirable for high performance optical delay lines, optical buffers, and optical storage. As the slow light in the PC-CROW is based on the weak coupling of the localized mode between the microcavities, the microcavities have a significant impact on the slow light properties in PC-CROW structures [12, 13].

To produce slow light in a PC-CROW is easy, but the high group index may be accompanied by a very narrow band and high dispersion. Many researchers have achieved a wide band and low dispersion by adjusting the radius of the holes and the size of the microcavities, changing the distance between adjacent microcavities, and shifting the locations of surrounding rods [14–17]. However, it is not easy to obtain the ultra-slow-light effect with a relative wideband, especially with a group index of $n_g > 10^2$.

In our previous study, we introduced eye-shaped scatterers into PCWs instead of cylindrical holes on a silicon wafer, and we found that the width of the bandgap and the slow-light effect can be effectively adjusted by changing the parameters of the eye-shaped scatterers [18, 19]. In this study, we introduced eye-shaped scatterers into PC-CROWs and studied the slow-light effect of two-dimensional PC-CROW structures via the plane-wave expansion method (PWE). According to the principle of dispersion compensation, saddle-like curves between f and k can be obtained by adjusting the parameters of the scatterers, changing the parameters of the coupling microcavities and shifting the positions of the scatterers such that both positive dispersion and negative dispersion coexist and offset each other. As a result, the total dispersion of the structure can be subtractive by the compensation of the positive dispersion and negative dispersion, and slow light with decent flat band and group index can be achieved by optimizing the parameters.

2 Theory and design

The established relationship between the dispersion and n_g is described as follows:

$$n_g = \frac{c}{v_g} = c\frac{\mathrm{d}k}{\mathrm{d}\omega} = n_{eff} + \omega\frac{\mathrm{d}n_{eff}}{\mathrm{d}\omega}, \quad (1)$$

where n_{eff} is the effective index, and ω is the central angular frequency of the incident pulse. n_{eff} and ω can be substituted by the wave number $k = 2\pi n_{eff}/\lambda$, where λ is the operating wavelength, and $f = \omega a/(2\pi c)$ is the normalized frequency. For slow light, $n_g \gg n_{eff}$, and Eq. (2) can be derived from Eq. (1), whereby we can obtain n_g in specific frequency regions where f varies with k [21]:

$$n_g = \frac{a}{2\pi}\frac{\mathrm{d}k}{\mathrm{d}f}. \quad (2)$$

Obviously, n_g is the slope of the curve f versus k: (i) For a line-defect waveguide, we can easily find large linear regions and then seek the different n_g curves; thus, many researches usually adopt zero-dispersion theory for line-defect waveguides, as it can achieve slow light with a wide band, very low dispersion, and a small value of the group index n_g. (ii) For PC-CROW structures, it is not easy to obtain large linear regions. The nonlinear curve may result in a high group index n_g in a very narrow region, and this phenomenon can be explained by the principle of dispersion compensation, because there is positive dispersion and negative dispersion.

For comparison, the PC-CROW structures used are triangular lattice rods on a silicon wafer ($n_{si} = 3.46$) with the same lattice parameter $a = 1$ μm (since n_g is not determined by it), and eye-shaped scatterers are employed [4, 19, 22] with the parameters b and c representing the radii of the major and minor axes of the eye-shaped scatterers, respectively. We define the parameter $e = 1 - c/b$, which ranges from 0 to 1. This parameter describes the degree of deviation of the eye-shape from a circle and is chosen, because the ratio of b to c has a larger effect on the shape of the eye-shape and thus the optical properties of the scatterers than the individual values b or c.

For better slow light, the transverse shifting parameter ds of the microcavities was needed, which was often compared with the lattice parameter a as shown in the figures. In the supercell calculation, according to the PWE method, we selected the number of plane waves in each axis as 32 and the eigenvalue tolerance as 10^{-8}, for sufficient calculation precision.

Figure 1(a) shows the relationship between f and k for the line-defect waveguide. Figure 1(b) shows the curve

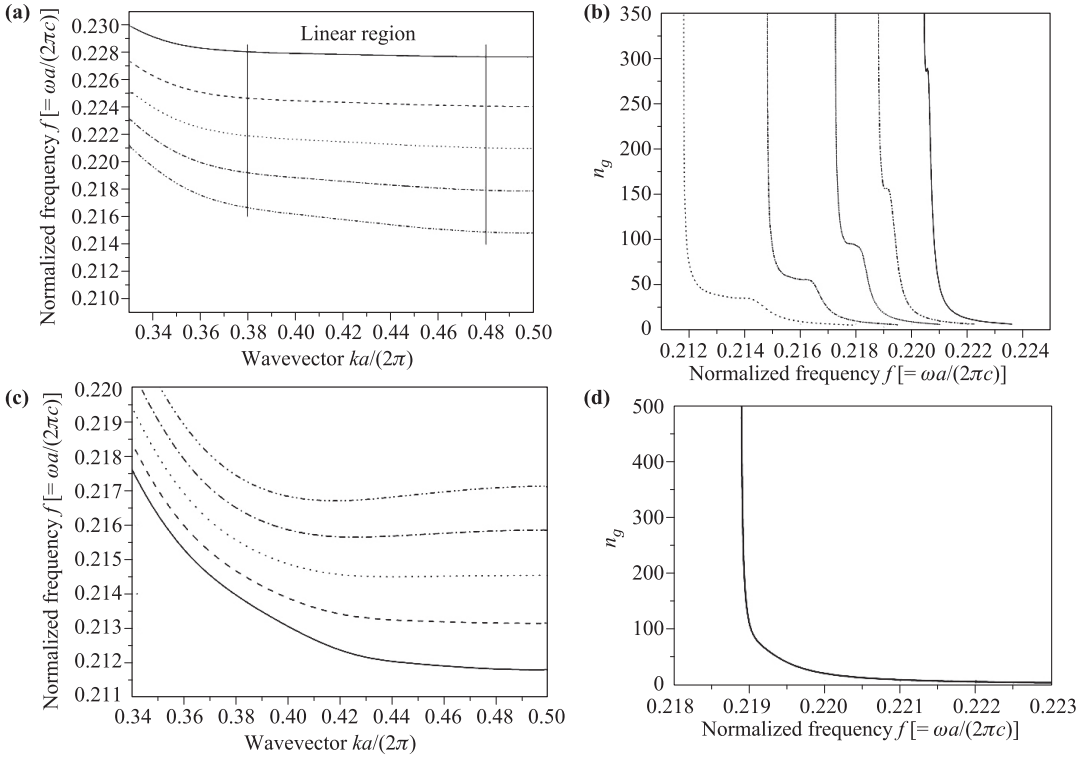

Fig. 1 **(a)** Relationship between f and k for the line-defect waveguide. **(b)** Curve of the group index n_g versus f for the line-defect waveguide. **(c)** Relationship between f and k for the PC-CROW structure. **(d)** Curve of the group index n_g versus f for the PC-CROW structure.

of the group index n_g versus f for the line-defect waveguide. Figure 1(c) shows the relationship between f and k for the PC-CROW structure. Figure 1(d) shows the curve of group index n_g versus f for the PC-CROW structure. From Figs. 1(a) and (c), we can see clearly that large linear dispersion region can be obtained in the line-defect waveguide, but it is very difficult to acquire slow light with flat wideband in the PC-CROW structure. From Figs. 1(b) and (d), we know that the value of the group index n_g is very small for the line-defect waveguide; therefore, the group velocity is relatively large. However, a high group refractive index may be achieved in the PC-CROW structure. Therefore, the group velocity is low in the PC-CROW structure.

Another problem is the criterion for the evaluation of the PC-CROW. The concept of the normalized delay bandwidth product (NDBP) was first introduced for a line-defect waveguide as follows [20]:

$$NDBP = n_g \Delta\omega/\omega_0, \tag{3}$$

where $\Delta\omega$ is the bandwidth with a central frequency of ω_0. In most research, a bandwidth criterion was selected where n_g varies within a 5% or 10% range for the line-defect waveguide. However, there is a problem for the PC-CROW structure, as its n_g varies quickly, and it is difficult to obtain a flat wideband. Some studies used the entire bandwidth as $\Delta\omega$ [20]; for example, Zhu adapted the average group index as per Eq. (4) and substituted it for the group index in Eq. (3) [21]:

$$\bar{n}_g = \int_{\omega_0}^{\omega} n_g(\omega)\mathrm{d}\omega/\Delta\omega. \tag{4}$$

To achieve slow light with a high group index and decent flat band in the PC-CROWs, we should let the positive dispersion and negative dispersion offset each other. There are two steps for effectively achieving that: first search for saddle-like curves between f and k, and then optimize the parameters to obtain ideal curves between f and n_g.

3 Simulations

3.1 Model 1: PC-CROW structure with (2 + 2) microcavities

Figure 2(a) shows a schematic of a PC-CROW structure with (2 + 2) microcavities. Figure 2(b) shows the curve of f versus k with different values of e, with fixed values of $b/a = 0.38$ and $\mathrm{d}s/a = 0.305$. Figure 2(c) shows the curve of f versus k with different values of $\mathrm{d}s$, with fixed values of $b/a = 0.38$ and $e = 0.40$. Figure 2(d) shows the curve of n_g versus f with the optimal parameters: $b/a = 0.38$, $e = 0.40$, and $\mathrm{d}s/a = 0.305$, where n_g increases first and then decreases rapidly as f increases from 0.2130 to

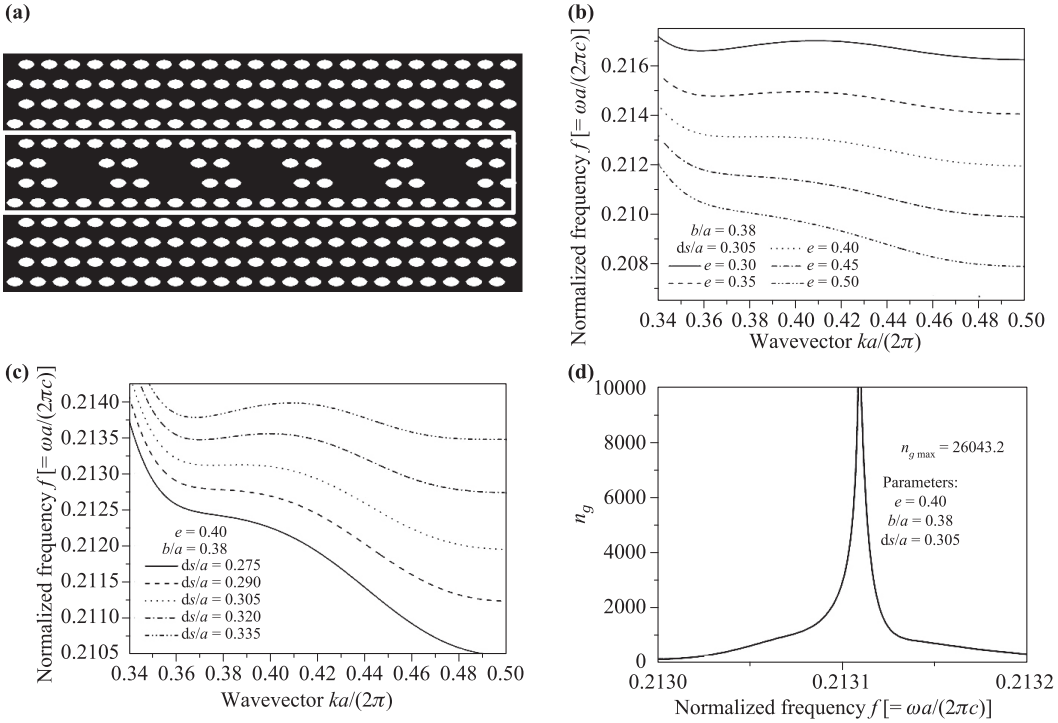

Fig. 2 **(a)** Schematic of the PC-CROW structure with (2 + 2) microcavities. **(b)** Curve of f versus k with different values of e. **(c)** Curve of f versus k with different values of $\mathrm{d}s$. **(d)** Curve of n_g versus f with the optimal parameters.

0.2132. A maximum n_g of approximately 2.6×10^4 can be observed when $f \approx 0.21313$.

3.2 Model 2: PC-CROW structure with $(2+1+2)$ microcavities

Figure 3(a) shows a schematic diagram of the PC-CROW structure with (2+1+2) microcavities. Figure 3(b) shows the curve of f versus k with different values of e, with fixed values of $b/a = 0.43$ and $\mathrm{d}s/a = 0.325$. Figure 3(c) shows the curve of f versus k with different values of $\mathrm{d}s$, with fixed values of $b/a = 0.43$ and $e = 0.40$. Figure 3(d) shows the curve of n_g versus f with the optimal parameters: $b/a = 0.43$, $e = 0.40$, and $\mathrm{d}s/a = 0.325$. Here, n_g increases first and then decreases rapidly as f increases from 0.2246 to 0.2248, and a maximum n_g of approximately 5.7×10^4 is observed when $f \approx 0.22474$.

3.3 Model 3: PC-CROW structure with more complicated microcavities

Figure 4(a) shows a schematic of a PC-CROW structure with more complicated microcavities, i.e., $(2+1+2)$ microcavities. Figure 4(b) shows the curve of f versus k with different values of e, with fixed values of $b/a = 0.43$ and $\mathrm{d}s/a = 0.103$. Figure 4(c) shows the curve of f versus k with different values of $\mathrm{d}s$, with fixed values of $b/a = 0.43$ and $e = 0.40$. Figure 4(d) shows the curve of n_g versus f with the optimal parameters: $b/a = 0.43$, $e = 0.40$, and $\mathrm{d}s/a = 0.103$. Here, n_g increases first and subsequently decreases rapidly as f increases from 0.2232 to 0.2234, and a maximum n_g of approximately 1.26×10^4 is observed when $f \approx 0.22324$.

4 Results and discussion

Most curves of f and k do not exhibit a saddle-like mode, which has great influence on the slow-light effect of PC-CROW structures. Figure 5(a) shows a schematic diagram of a PC-CROW structure with $(2+3+2)$ microcavities. Figure 5(b) shows the curve of f versus k with different values of e, for the structure in Fig. 5(a). Figure 5(c) shows a schematic of a PC-CROW structure with revolving scatterers. Figure 5(d) shows the curve of f versus k with different values of e, for the structure in Fig. 5(c). Although the microcavities in Figs. 5(a) and (c) differ significantly, they are symmetrical structures, and neither of them changes the arrangement of the triangular lattice. Their curves of f versus n_g decrease monotonically and rapidly, and their bandwidths of slow light are very small, similar to that in Fig. 1(d).

In fact, asymmetry is effective for obtaining a saddle-like curve, as shown in Figs. 2(a), 3(a), and 4(a), in

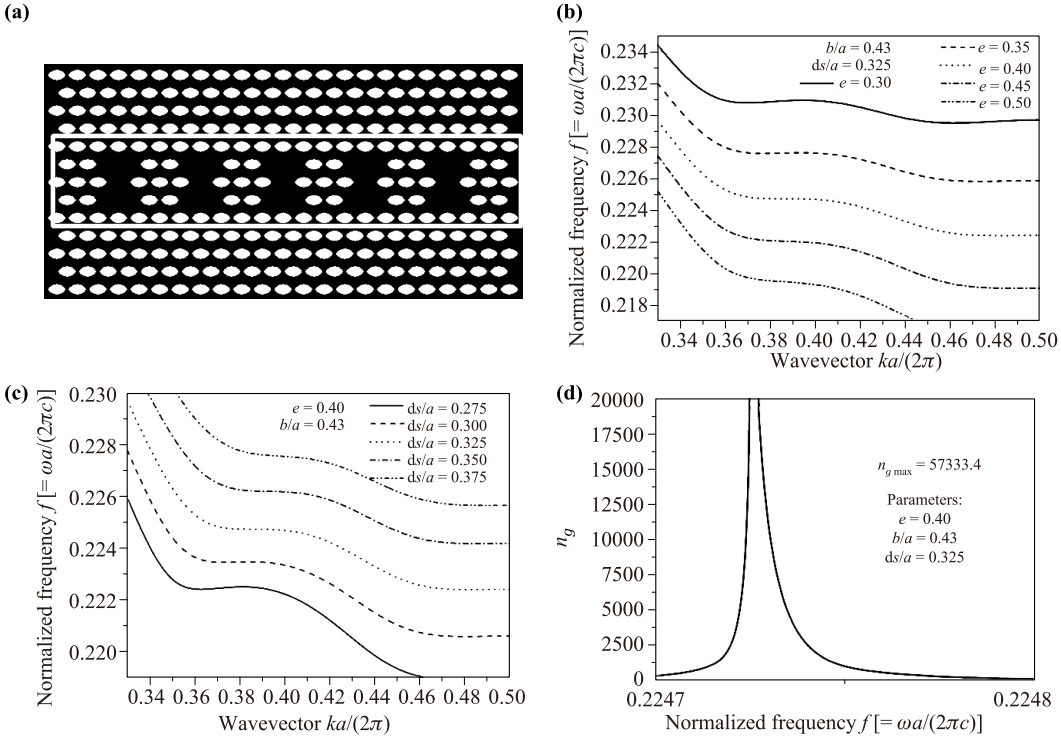

Fig. 3 **(a)** Schematic of the PC-CROW structure with $(2+1+2)$ microcavities. **(b)** Curve of f versus k with different values of e. **(c)** Curve of f versus k with different values of $\mathrm{d}s$. **(d)** Curve of n_g versus f with the optimal parameters.

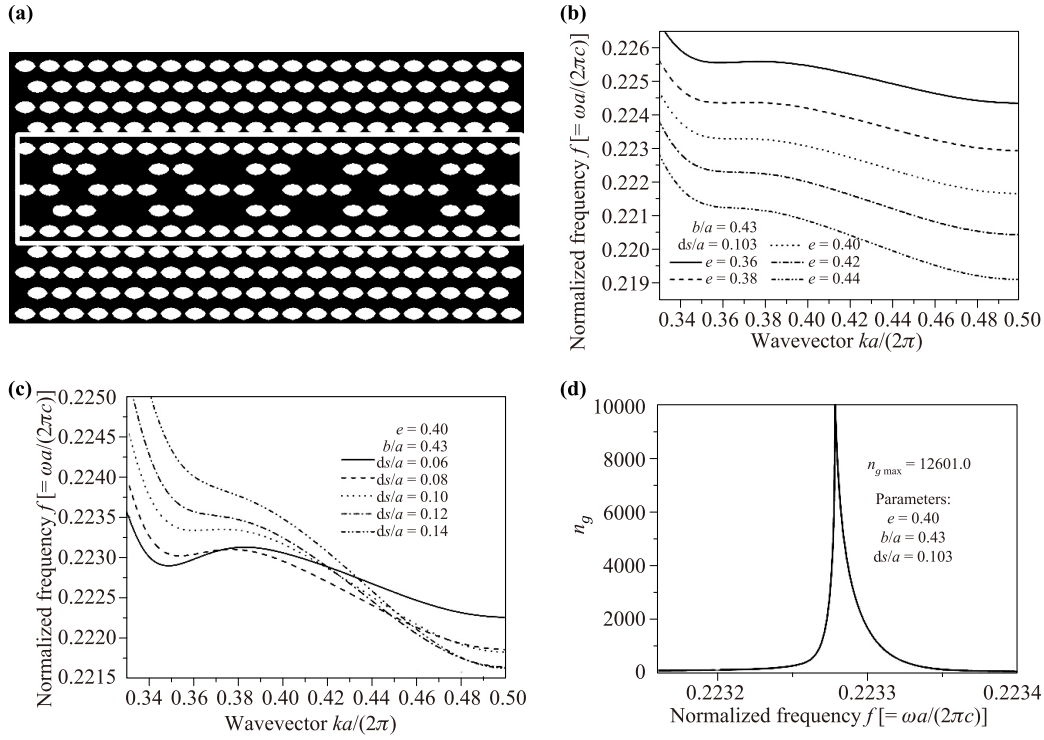

Fig. 4 **(a)** Schematic of the PC-CROW structure with more complicated microcavities. **(b)** Curve of f versus k with different values of e. **(c)** Curve of f versus k with different values of ds. **(d)** Curve of n_g versus f with the optimal parameters.

which the bandwidth of slow light can increase significantly while the peak value of the group refractive index n_g remains the same or even increases. We can use the principle of dispersion compensation: the mechanism for the saddle-like mode involves three kinds of dispersions in the dispersion curve: positive dispersion, negative dispersion, and flat-band dispersion, the former part can be compensated by the latter part, there is small dispersion overall and less signal distortion after the compensation in the transmission process, and the structure has an improved slow-light effect.

Second, adjusting both the parameters of the scatterers and the positions of the microcavities is useful for optimizing the PC-CROW structure to obtain ideal curves between f and n_g. The maximum values of n_g, with corresponding frequencies and optimal parameters, are shown in Table 1. The structures can achieve extremely high group refractive indices, all of which exceed 10^4, and higher group refractive index with lower dispersion can be achieved by further fine-tuning of the parameters.

Third, as mentioned in the second part of the paper, the concept of the NDBP was first introduced for a line-defect waveguide, and most researchers selected a bandwidth criterion where n_g varies within a 5% or 10% range for the line-defect waveguide. It is better that there is a threshold for the group index, such as $n_g > 10^2$ or $n_g > 10^3$, because the advantage of PC-CROW structures is their high group index. Thus, we prefer to adopt the maximum value of the high group index $n_{g\,\max}$ to replace the average group index and choose $\Delta\omega_x$ as the bandwidth of $n_g > 10^2$ or $n_g > 10^3$. There is a new definition of N_x instead of the NDBP, as follows:

$$N_x = n_{g\,\max}\frac{\Delta\omega_x}{\omega_0}. \tag{5}$$

The new definition of N_x is significant, as a larger value of n_g means a lower group velocity, and a larger value of $\Delta\omega$ means better capacity of data transmission. We can use the normalized frequency f instead of ω, such that f_0 is the central frequency and Δf is the bandwidth of n_g larger than 10^2 or 10^3. The corresponding results of the slow-light properties are shown in Table 2.

The parameters, such as the maximum value of the high group index, central frequency, and bandwidth of n_g larger than 10^2 or 10^3, are listed in Table 2. More

Table 1 Optimal parameters and maximum group index for different models.

	b/a	e	ds/a	f_0	$n_{g\,\max}$
Model 1	0.38	0.40	0.305	0.21313	2.60×10^4
Model 2	0.43	0.40	0.325	0.22474	5.73×10^4
Model 3	0.43	0.40	0.103	0.22327	1.26×10^4

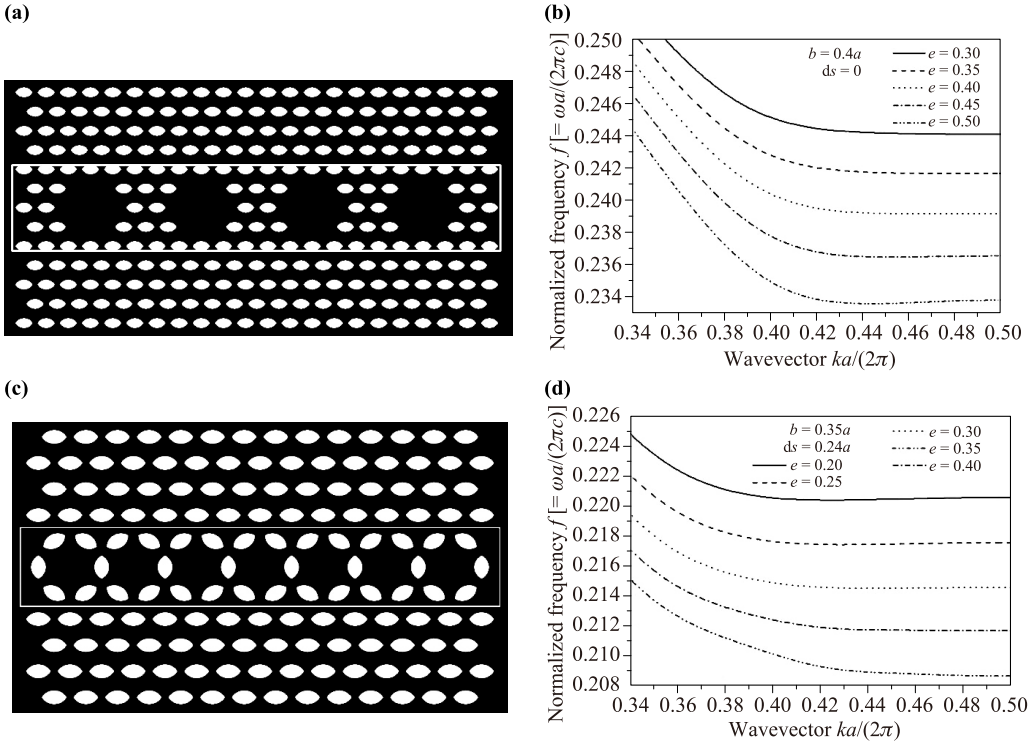

Fig. 5 **(a)** Schematic of a PC-CROW structure with $(2 + 3 + 2)$ microcavities. **(b)** Curve of f versus k with different values of e, for the structure in (a). **(c)** Schematic of a PC-CROW structure with revolving scatterers. **(d)** Curve of f versus k with different values of e, for the structure in (c).

Table 2 Three kinds of NDBPs for different models.

	$n_g(\times 10^4)$	f_0	$\Delta f_{100}(\times 10^{-4})$	$\Delta f_{1000}(\times 10^{-5})$	N_{100}	N_{1000}	NDBP
Model 1	2.60	0.21313	4.5	5.6	54.9	6.84	0.227
Model 2	5.73	0.22474	2.7	3.5	68.8	8.91	0.255
Model 3	1.26	0.22327	3.2	4.6	18.10	2.60	0.176

important are the three kinds of NDBPs in the different models: although they have the same order of magnitude, N_{100} and N_{1000} reveal the differences clearly and precisely. For example, when $n_g > 100$, N_{100} is 54.9, 68.8, and 18.10, and NDBP is 0.244, 0.255, and 0.176, respectively. The former provides a larger amount of information and more distinctive information for the three kinds of models.

Finally, although our research consists of theoretical analysis and simulation, we wish to mention the acceptable tolerance of fabrication. Some researchers worry that the fabrication error may reduce the slow-light effect because it is sensitive to the parameters. Because the acceptable tolerance of fabrication is ±10 nm, the PCW structures can be enlarged or reduced proportionally according to the operating wavelength, and the fabrication tolerance is sufficient for practical applications for millimeter waves and terahertz waves, as those in our previous research [19], and the fabrication error will continue to decrease with technological developments.

5 Summary

There are two steps to effectively obtain slow light with high group index and wideband in PC-CROW structures. One of them is to search for the saddle-like mode between f and k, and then optimize the parameters to obtain ideal curves between f and n_g. We can achieve slow light with a large group index by choosing asymmetric scatterers and adjusting their parameters, as well as by changing the periodic arrays of the scatterers. The simulations show that the PC-CROW structures can easily achieve a maximum group index larger than 10^4, which means that the group velocity is less than $10^{-4}c$.

In addition, the slow-light mechanism for PC-CROWs

differs from that of line-defect waveguides, and NDBP was first introduced for line-defect waveguides. In the majority of previous research on this topic, a bandwidth criterion was selected where n_g varies within a 5% or 10% range for the line-defect waveguide. We suggest an NDBP with a new varying range of $n_g > 10^2$ or $n_g > 10^3$ as a new and effective criterion for evaluating PC-CROWs, which can provide a greater and more distinctive information about the slow light effect in PC-CROWs.

Acknowledgements This work was supported by the National Natural Science Foundation of China (Grant No. 11144007) and the Natural Science Foundation of Shandong Province (Grant No. ZR2016AM27).

References

1. R. S. Tucker, P. C. Ku, and C. J. Chang-Hasnain, Slow-light optical buffers: Capabilities and fundamental limitations, *J. Lightwave Technol.* 23(12), 4046 (2005)
2. S. K. Tripathy, S. Sahu, C. Mohapatro, and S. P. Dash, Implementation of optical logic gates using closed packed 2D-photonic crystal structure, *Opt. Commun.* 285(13–14), 3234 (2012)
3. K. Nozaki, A. Shinya, S. Matsuo, T. Sato, E. Kuramochi, and M. Notomi, Ultralow-energy and high-contrast all-optical switch involving Fano resonance based on coupled photonic crystal nanomicrocavities, *Opt. Express* 21(10), 11877 (2013)
4. Y. Wan, S. Ge, Y. Guo, and M. Yun, Application of 2D graded eye-shape scatterers for slow light effect in photonic crystal line-defect waveguide, *Optik (Stuttg.)* 125(5), 1605 (2014)
5. J. Chen, G. von Freymann, S. Choi, and G. Ozin, Amplified photochemistry with slow photons, *Adv. Mater.* 18(14), 1915 (2006)
6. Z. Cai, Z. Xiong, X. Lu, and J. Teng, In situ gold-loaded titania photonic crystals with enhanced photocatalytic activity, *J. Mater. Chem. A* 2(2), 545 (2014)
7. T. Baba, Slow light in photonic crystals, *Nat. Photon.* 2, 465 (2008)
8. A. C. Liapis, Optimizing photonic crystal waveguides for on-chip spectroscopic applications, *Opt. Express* 21(8), 10160 (2013)
9. S. A. Schulz, L. O'Faolain, D. M. Beggs, T. P. White, A. Melloni, and T. F. Krauss, Dispersion engineered slow light in photonic crystal: A comparison, *J. Opt.* 12(10), 104004 (2010)
10. A. Yariv, Y. Xu, R. K. Lee, and A. Scherer, Coupled-resonator optical waveguide: A proposal and analysis, *Opt. Lett.* 24(11), 711 (1999)
11. K. Sakai, E. Miyai, and S. Noda, Two-dimensional coupled wave theory for square-lattice photonic-crystal lasers with TM-polarization, *Opt. Express* 15(7), 3981 (2007)
12. E. Waks and J. Vuckovic, Coupled mode theory for photonic crystal cavity-waveguide interaction, *Opt. Express* 13(13), 5064 (2005)
13. H. Tian, F. Long, W. Liu, and Y. Ji, Tunable slow light and buffer capability in photonic crystal coupled-microcavity waveguides based on electro-optic effect, *Opt. Commun.* 285(10–11), 2760 (2012)
14. K. Tian, W. Arora, S. Takahashi, J. Hong, and G. Barbastathis, Dynamic group velocity control in a mechanically tunable photonic-crystal coupled-resonator optical waveguide, *Phys. Rev. B* 80(13), 134305 (2009)
15. K. Üstün and H. Kurt, Ultra slow light achievement in photonic crystals by merging coupled cavities with waveguides, *Opt. Express* 18(20), 21155 (2010)
16. N. Matsuda, E. Kuramochi, H. Takesue, and M. Notomi, Dispersion and light transport characteristics of large-scale photonic-crystal coupled nanomicrocavity arrays, *Opt. Lett.* 39(8), 2290 (2014)
17. H. Kurt, M. Turduev, and I. H. Giden, Crescent shaped dielectric periodic structure for light manipulation, *Opt. Express* 20(7), 7184 (2012)
18. Y. Wan, Z. Cai, Q. Li, and X. S. Zhao, Simulation and fabrication of THz waveguides with silicon wafer by using eye-shaped pillars as building blocks, *Appl. Phys. A* 102(2), 373 (2011)
19. Y. Wan, K. Fu, C. H. Li, and M. J. Yun, Improving slow light effect in photonic crystal line-defect waveguide by using eye-shaped scatterers, *Opt. Commun.* 286, 192 (2013)
20. C. Li, R. Su, Y. Wang, and X. Zhang, Theoretical study of ultra-wideband slow light in dual-stub-coupled plasmonic waveguide, *Opt. Commun.* 377, 10 (2016)
21. N. Zhu, Y. Y. Li, C. C. Chen, and S. Yan, Slow light in dual-periodic photonic crystals based slotted-waveguide coupled cavity, *Opt. Laser Technol.* 83, 125 (2016)
22. Y. Wan, X. Ge, S. Xu, Y. Guo, and F. Yuan, Ultra-slow light effects in symmetric and asymmetric waveguide structures with moon-like scatterers, *Front. Phys.* 12(1), 124204 (2017)